Analysis. Averaged EPSCs (average of 3 or 5) were digitally filtered at 1 kHz and fitted with one or two exponentials using SigmaPlot 3.0. Each EPSC was fit with both a single and a double exponential to determine which was the best fit. For the LTP experiments and interleaved controls, EPSC averages were constructed from all EPSCs collected during baseline (average of 50–100) and after LTP (typically an average of 300–600) or after the control manipulation. Only the data collected at room temperature were included in the kinetic analysis. For I–V analysis, holding potentials of −70, −50, −30, −10, 10, 30 and 50 mV were used; for the dual component EPSCs, separate amplitude measurements were made at the peak and at the tail ($5–6 \times \tau_{fast}$ from the peak). Fits for the I–V data were obtained using linear regression analysis (SigmaPlot 3.0); first order for peak of dual component EPSC, third order for dual EPSC tail and kainate EPSC peak. Two rectification indices were calculated for each I–V series; a ratio of the conductance (I_{EPSC}/V) for currents at +30 and −70 mV, and a ratio for +50 and −50 mV. The mean rectification index for +40 versus −60 mV was estimated by averaging the mean index values for the two sets of potentials (this allowed a direct comparison with data from ref. 20). Spontaneous EPSC traces were constructed by aligning 10–20 events to the point of fastest rise by eye and averaging. Charge transfer through the AMPAR- and KAR-mediated components of the dual-component EPSCs were estimated by calculating the product of τ and the current at peak obtained from the exponential fits. All values are expressed as mean ± s.e.m. Statistical significance was assessed using two-tailed paired or unpaired Student's t-tests as appropriate ($P < 0.05$ considered significant).

Drugs. The active isomer of GYKI 53655 was used in all experiments (supplied by Eli Lilly). D-AP5, CNQX (Tocris) and picrotoxin (Sigma) were obtained commercially.

Received 6 May; accepted 15 June 1999.

1. Hollmann, M. & Heinemann, S. Cloned glutamate receptors. *Annu. Rev. Neurosci.* **17,** 31–108 (1994).
2. Bettler, B. & Mulle, C. Neurotransmitter receptors II. AMPA and kainate receptors. *Neuropharmacology* **34,** 123–139 (1995).
3. Bleakman, D. & Lodge, D. Neuropharmacology of AMPA and kainate receptors. *Neuropharmacology* **37,** 1187–1204 (1998).
4. Chittajallu, R., Braithwaite, S. P., Clarke, V. R. J. & Henley, J. M. Kainate receptors: subunits, synaptic localisation and function. *Trends Pharmacol. Sci.* **20,** 26–35 (1999).
5. Chittajallu, R. *et al.* Regulation of glutamate release by presynaptic kainate receptors in the hippocampus. *Nature* **379,** 78–81 (1996).
6. Clarke, V. R. J. *et al.* A hippocampal GluR5 kainate receptor regulating inhibitory synaptic transmission. *Nature* **389,** 599–603 (1997).
7. Rodríguez-Moreno, A., Herreras, O. & Lerma, J. Kainate receptors presynaptically downregulate GABAergic inhibition in the rat hippocampus. *Neuron* **19,** 893–901 (1997).
8. Castillo, P. E., Malenka, R. C. & Nicoll, R. A. Kainate receptors mediate a slow postsynaptic current in hippocampal CA3 neurons. *Nature* **388,** 182–186 (1997).
9. Vignes, M. & Collingridge, G. L. The synaptic activation of kainate receptors. *Nature* **388,** 179–182 (1997).
10. Cossart, R., Esclapez, M., Hirsch, J. C., Bernard, C. & Ben-Ari, Y. GluR5 kainate receptor activation in interneurons increases tonic inhibition of pyramidal cells. *Nature Neurosci.* **1,** 470–478 (1998).
11. Frerking, M., Malenka, R. C. & Nicoll, R. A. Synaptic activation of kainate receptors on hippocampal interneurons. *Nature Neurosci.* **1,** 479–486 (1998).
12. Li, H. & Rogawski, M. A. GluR5 kainate receptor-mediated synaptic transmission in rat basolateral amygdala in vitro. *Neuropharmacology* **37,** 1279–1286 (1998).
13. DeVries, S. H. & Schwartz, E. A. Kainate receptors mediate synaptic transmission between cones and 'Off' bipolar cells in a mammalian retina. *Nature* **397,** 157–160 (1999).
14. Li, P. *et al.* Kainate-receptor-mediated sensory synaptic transmission in mammalian spinal cord. *Nature* **397,** 161–164 (1999).
15. Paternain, A. V., Morales, M. & Lerma, J. Selective antagonism of AMPA receptors unmasks kainate receptor-mediated responses in hippocampal neurons. *Neuron* **14,** 185–189 (1995).
16. Wilding, T. J. & Huettner, J. E. Differential antagonism of alpha-amino-3-hydroxy-5-methyl-4-isozolepropionic acid-preferring and kainate-preferring receptors by 2,3-benzodiazepines. *Mol. Pharmacol.* **47,** 582–587 (1995).
17. Ruano, D., Lambolez, B., Rossier, J., Paternain, A. V. & Lerma, J. Kainate receptor subunits expressed in single cultured hippocampal neurons: molecular and functional variants by RNA editing. *Neuron* **14,** 1009–1017 (1995).
18. Bowie, D. & Mayer, M. L. Inward rectification of both AMPA and kainate subtype glutamate receptors is generated by polyamine-mediated ion channel block. *Neuron* **15,** 453–462 (1995).
19. Kamboj, S. K., Swanson, G. T. & Cull-Candy, S. G. Intracellular spermine confers rectification on rat calcium-permeable AMPA and kainate receptors. *J. Physiol.* **486,** 297–303 (1995).
20. Tóth, K. & McBain, C. J. Afferent-specific innervation of two distinct AMPA receptor subtypes on single hippocampal interneurons. *Nature Neurosci.* **1,** 572–578 (1998).
21. Washburn, M. S., Numberger, M., Zhang, S. & Dingledine, R. Differential dependence on GluR2 expression of three characteristic features of AMPA receptors. *J. Neurosci.* **17,** 9393–9406 (1997).
22. Fox, K. The critical period for long-term potentiation in primary sensory cortex. *Neuron* **15,** 485–488 (1995).
23. Crair, M. C. & Malenka, R. C. A critical period for long-term potentiation at thalamocortical synapses. *Nature* **375,** 325–328 (1995).
24. Isaac, J. T. R., Crair, M. C., Nicoll, R. A. & Malenka, R. C. Silent synapses during development of thalamocortical inputs. *Neuron* **18,** 269–280 (1997).
25. Feldman, D. E., Nicoll, R. A., Malenka, R. C. & Isaac, J. T. R. Long-term depression at thalamocortical synapses in developing rat somatosensory cortex. *Neuron* **21,** 347–357 (1998).
26. Kullmann, D. M. & Asztély, F. Extrasynaptic glutamate spillover in the hippocampus: evidence and implications. *Trends Neurosci.* **21,** 8–14 (1998).
27. Paternain, A. V., Rodriguez-Moreno, A., Villarroel, A. & Lerma, J. Activation and desensitisation properties of native and recombinant kainate receptors. *Neuropharmacology* **37,** 1249–1260 (1998).
28. Patneau, D. K. & Mayer, M. L. Structure–activity relationships for amino acid transmitter candidates acting at *N*-methyl-D-aspartate and quisqualate receptors. *J. Neurosci.* **10,** 2385–2399 (1990).
29. Rozov, A., Zilberter, Y., Wollmuth, L. P. & Burnashev, N. Facilitation of currents through rat Ca^{2+}-permeable AMPA receptor channels by activity-dependent relief from polyamine block. *J. Physiol.* **511,** 361–377 (1998).
30. Agmon, A. & Connors, B. W. Thalamocortical responses of mouse somatosensory (barrel) cortex *in vitro*. *Neuroscience* **41,** 365–379 (1991).

Acknowledgements. We thank G. Collingridge, V. Clarke, R. Chittajallu, S. Braithwaite and J. Crabtree for advice and comments; W. W. Anderson for providing the data acquisition software; and D. Lodge (Eli Lilly and Co.) for supplying the GYKI 53655. This work was supported by the Wellcome Trust.

Correspondence and requests for materials should be addressed to J.I.

Oligopeptide-repeat expansions modulate 'protein-only' inheritance in yeast

Jia-Jia Liu & Susan Lindquist

Howard Hughes Medical Institute, Department of Molecular Genetics and Cell Biology, University of Chicago, 5841 S. Maryland Avenue MC1028, Chicago, Illinois 60637, USA

The yeast [*PSI*$^+$] element represents a new type of genetic inheritance, in which changes in phenotype are transmitted by a 'protein only' mechanism[1–3] reminiscent of the 'protein-only' transmission of mammalian prion diseases[1,4]. The underlying molecular mechanisms for both are poorly understood and it is not clear how similar they might be. Sup35, the [*PSI*$^+$] protein determinant, and PrP, the mammalian prion determinant, have different functions, different cellular locations and no sequence similarity; however, each contains five imperfect oligopeptide repeats—PQGGYQQYN in Sup35 and PHGGGWGQ in PrP[5,6]. Repeat expansions in PrP produce spontaneous prion diseases[7,8]. Here we show that replacing the wild-type *SUP35* gene with a repeat-expansion mutation induces new [*PSI*$^+$] elements, the first mutation of its type among these newly described elements of inheritance. *In vitro*, fully denatured repeat-expansion peptides can adopt conformations rich in β-sheets and form higher-order structures much more rapidly than wild-type peptides. Our results provide insight into the nature of the conformational changes underlying protein-based mechanisms of inheritance and suggest a link between this process and those producing neurodegenerative prion diseases in mammals.

The Sup35 protein of *Saccharomyces cerevisiae* is a subunit (eRF3) of the eukaryotic release factor[9,10]. In [*PSI*$^+$] cells, most of the Sup35 protein is sequestered into higher-order protein complexes and is unavailable to function in translation termination[2,3]. Once formed, these complexes are self-perpetuating and are passed from mother cells to daughters. As a result, [*PSI*$^+$] causes a heritable change in the fidelity of protein synthesis: ribosomes have an increased tendency to read through stop codons, and nonsense mutations are suppressed. Certain point mutations and deletions in the amino-terminal prion-determining domain of Sup35 (NPD) are defective in the production of higher-order Sup35 complexes and in the propagation of [*PSI*$^+$][11–14]. To investigate the importance of the oligopeptide repeats in this region, we created one variant with the last four repeats deleted (RΔ2–5) and another with two additional copies of the second repeat (R2E2). The wild-type gene was replaced by the genes encoding these variants, in its normal chromosomal context, by homologous recombination in isogenic [*PSI*$^+$] and [*psi*$^-$] cells. Western blotting confirmed that all three proteins accumulated to the same extent.

First, we assayed the spontaneous appearance of new [*PSI*$^+$] elements in [*psi*$^-$] strains. The *ade1–14* allele, which contains a

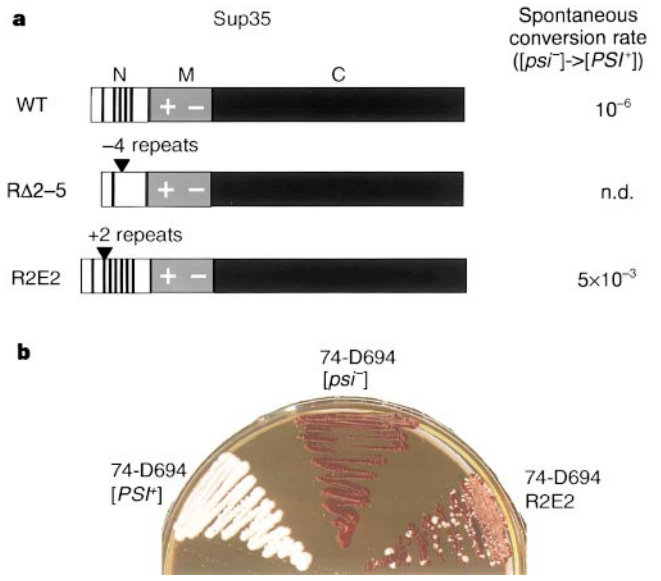

Figure 1 Effect of the R2E2 and RΔ2–5 mutations on spontaneous conversion from [*psi*⁻] to [*PSI*⁺]. **a**, Diagrams of wild-type (WT) and mutant Sup35 and table of conversion rates determined by plating cells on SD-Ade medium. Vertical lines in the N-terminal region of Sup35 (N) represent oligopeptide repeats. The highly charged nature of the middle region (M) is indicated. The C-terminal region (C) functions in translation termination. n.d., no guanidine HCl-curable Ade⁺ cells were detected in $>10^8$ cells plated. **b**, White [*PSI*⁺] colonies appear at a high rate when [*psi*⁻] cells with an R2E2/SUP35 replacement are streaked on YPD.

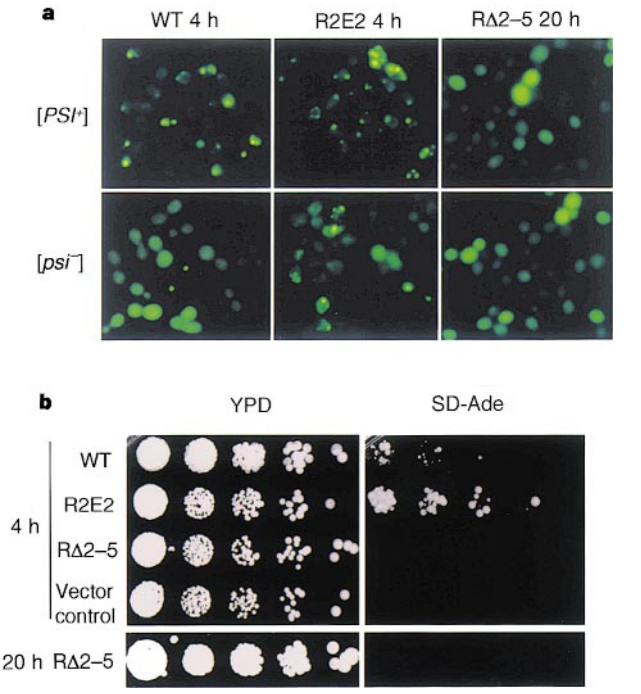

Figure 2 Visualization of [*PSI*⁺] conversions. **a**, Fluorescence of NM–GFP fusion proteins in [*PSI*⁺] and [*psi*⁻] cells after 4 h (wild-type (WT) NM–GFP and R2E2 NM–GFP) and 20 h (RΔ2–5 NM–GFP) of induction. **b**, Induction of heritable [*PSI*⁺] factors. [*psi*⁻] cells analysed in **a** were serially diluted in 5-fold increments and spotted onto YPD medium, to measure total cells in the culture, and SD-Ade medium, to measure [*PSI*⁺] cells. Control construct, GFP alone.

nonsense mutation in the auxotrophic marker *ADE1*, provides a particularly convenient method for monitoring the appearance of [*PSI*⁺]. The suppression of *ade1–14* allows cells to grow on adenine-deficient synthetic medium (SD-Ade) and prevents the accumulation of metabolic by-products that cause colonies to appear red on rich medium (YPD)[12,15]. Wild-type cells of strain 74-D694 rarely produced colonies on SD-Ade medium (frequency was approximately one per 10^6 cells plated) and rarely produced white colonies on rich medium (Fig. 1). RΔ2–5 cells produced such colonies at an even lower frequency (less than 1 in 10^8 cells); none of these was due to the appearance of [*PSI*⁺], because they could not be cured by growth on medium containing 5 mM guanidine hydrochloride[16]. In striking contrast, R2E2 cells frequently produced colonies on SD-Ade medium (~5,000 times more frequently than wild-type cells), and similarly increased the spontaneous appearance of white colonies on rich medium (Fig. 1). Growth on medium containing guanidine-HCl cured both the ability of the cells to grow on SD-Ade medium and the white colony colour on rich medium, confirming that the phenotypes were due to the appearance of genuinely new [*PSI*⁺] elements.

Next we examined the effects of the repeat variants when they replaced the wild-type *SUP35* gene in cells that were already [*PSI*⁺]. Cells with the R2E2 replacement remained [*PSI*⁺]. All cells carrying the RΔ2–5 replacement became [*psi*⁻] (data not shown). Thus, the oligopeptide repeats are crucial for the maintenance of [*PSI*⁺].

Two defining features of the [*PSI*⁺] phenomenon are that transient overexpression of fragments carrying the N-terminal region of Sup35 is sufficient to induce heritable new [*PSI*⁺] elements[11,12,17], and the appearance of [*PSI*⁺] is associated with the formation of higher-order complexes of Sup35[2,3,13,14]. We examined whether transient expression of N-terminal fragments containing the repeat variants could induce new [*PSI*⁺] elements in wild-type cells, and also whether this would correlate with the appearance of new protein complexes. To do this, we used a fusion between NM, the N-terminal and middle domains of Sup35 (amino acids 1–253), and green fluorescent protein (NM–GFP). In [*PSI*⁺] cells, newly synthesized NM–GFP rapidly coalesces into intense fluorescent foci as it joins pre-existing complexes of Sup35[2]. In [*psi*⁻] cells, NM–GFP is initially soluble, but prolonged expression produces intense fluorescent foci coincident with the formation of new [*PSI*⁺] elements[2].

Plasmids encoding inducible wild-type and repeat-variant NM–GFPs were transformed into isogenic [*PSI*⁺] and [*psi*⁻] cells with a wild-type *SUP35* gene in the chromosome. RΔ2–5 NM–GFP produced no intense fluorescent foci in either [*PSI*⁺] or [*psi*⁻] cells even after 20 h of induction. Both R2E2 NM–GFP and wild-type NM–GFP produced intense foci in virtually all [*PSI*⁺] cells after only 4 h of induction (Fig. 2a). New fluorescent foci appeared in [*psi*⁻] cells at a higher frequency with R2E2 NM–GFP than with wild-type NM–GFP at both 4 and 20 h (Fig. 2a, and data not shown). To monitor the appearance of new [*PSI*⁺] elements in the [*psi*⁻] cells, they were plated onto media selective for [*PSI*⁺] but not for the plasmids. No [*PSI*⁺] colonies developed from cultures that had expressed RΔ2–5 NM–GFP for 20 h (Fig. 2b). Cells expressing R2E2 NM–GFP for 4 and 20 h produced ~5-fold as many [*PSI*⁺] colonies as cells expressing wild-type NM–GFP (Fig. 2b, and data not shown).

The results suggest that the oligopeptide repeat expansion increases the spontaneous appearance of new [*PSI*⁺] elements by facilitating the initial conformational conversion of Sup35 protein and directly influencing the conversion of newly made protein. But it remains possible that R2E2 NM increases the appearance of [*PSI*⁺] elements indirectly by affecting the physiology of the cell in a manner that in turn influences the independent folding of other Sup35 molecules. (Indeed, this is a caveat for all previous investigations examining the conversion of [*psi*⁻] cells to [*PSI*⁺].) To determine whether proteins expressed from the plasmids interact directly with endogenous Sup35, we used a GFP antibody and immunomagnetic beads to extract proteins associated with the GFP

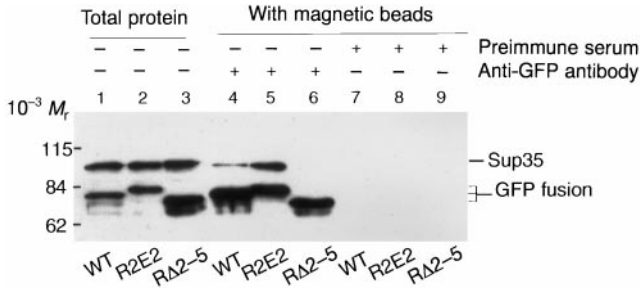

Figure 3 Interactions between endogenous full-length Sup35 and GFP-fusion proteins. [*psi*$^-$] cells were induced to express NM–GFP proteins with $CuSO_4$ for 4 h. GFP-fusion proteins were extracted from yeast cell lysates by purification with immunomagnetic beads by using an anti-GFP antibody. Protein complexes were analysed by SDS–PAGE and immunoblotting with anti-Sup35 1B antibody. Lanes 1–3, total proteins in the lysate; lanes 4–6, proteins bound to magnetic beads in the presence of anti-GFP antibodies; lanes 7–9, proteins bound in the presence of preimmune serum. The positions of relative molecular mass (M_r) markers and of wild-type (WT) Sup35 and NM–GFP fusions are indicated.

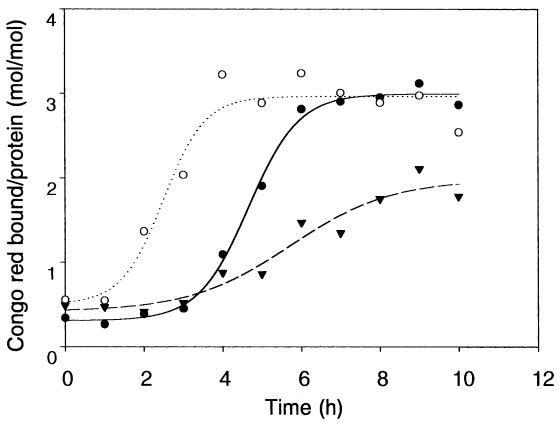

Figure 4 Kinetics of fibre formation of NM repeat mutants *in vitro*. Recombination proteins, wild-type (filled circles), R2E2 (open circles) or RΔ2–5 (triangles), purified from *Escherichia coli*[26] were diluted into aqueous buffer and the progression of fibre formation was monitored by the spectral shift produced on Congo-red binding[29]. Sigmoid regression analysis was done with Sigmaplot for Windows Version 4.01 (SPSS). Correlation coefficients: wild type, 0.9977; R2E2, 0.9749; RΔ2–5, 0.9720.

fusions from cell lysates. When wild-type NM–GFP was induced in [*psi*$^-$] cells for 4 h, some wild-type Sup35 was recovered on the beads (Fig. 3). With R2E2 NM–GFP, a larger fraction was recovered, and with RΔ2–5 NM–GFP, none. The increased appearance of new [*PSI*$^+$] elements in cells that express R2E2 NM–GFP is probably due to the protein's enhanced ability to self-assemble into higher-order complexes that can recruit and convert new Sup35 protein to the [*PSI*$^+$] state.

Next, we tested the effects of the repeat variants on the structural transitions of NM *in vitro*. When purified recombinant NM is denatured and diluted into aqueous buffers, it slowly changes from a random coil to a structure rich in β-sheets and forms fibres that bind Congo red, giving the spectral shift characteristic of amyloid proteins[13]. When deposited at high concentrations, these Congo-red-stained fibres also show apple-green birefringence (A. Cashikar and S.L., unpublished observations). The ability of preformed β-sheet-rich structures to promote the rapid conversion of soluble NM to the same state provides a simple molecular model for the propagation of [*PSI*$^+$] *in vivo*[13,14,18]. To determine whether the repeat variants alter the intrinsic capacity of the protein to fold into this form, we purified wild-type NM proteins and the repeat variants in the fully denatured state and diluted them into non-denaturing buffer. Structural changes were monitored by the binding of Congo red (Fig. 4) and confirmed by circular dichroism and electron microscopy (data not shown). The three proteins converted at profoundly different rates: the repeat expansion variant converted much more rapidly than the wild type, whereas the deletion variant converted much more slowly. The differences were obtained reproducibly in both rotated and unrotated reactions, although the rate of conversion in unrotated reactions was slower overall (data not shown). Thus, the mutations alter the intrinsic propensity of the protein, starting from the unfolded state to progress to a β-sheet-rich, more highly ordered structure.

Like the mammalian prion, [*PSI*$^+$] is believed to propagate by a 'protein only' mechanism. We find that an expansion of the oligopeptide repeats induces the spontaneous appearance of [*PSI*$^+$] and that deletion of the repeats eliminates it. Notably, certain mammalian prion diseases are linked to expansions of the oligopeptide repeats in PrP[7,8], and variants with reduced numbers of repeats are less susceptible to prion disease[19] (C. Weissmann, personal communication). The extraordinary similarity of the mutations that affect, on the one hand, the spontaneous appearance of a heritable proteinaceous element in yeast and, on the other hand, a heritable protein misfolding disease in mammals suggests a congruity in their underlying molecular mechanisms. In both fields, a major unanswered question is whether the acquisition of the prion state occurs through the structural rearrangement of native protein or through the diversion of transiently unfolded (or nascent) protein to an alternative folding pathway. Our experiments *in vitro* started with denatured protein. They therefore indicate that the rate at which higher-order, β-sheet-rich structure is acquired after the protein has reached the unfolded state can be a rate-limiting factor in the creation of new [*PSI*$^+$] elements. PrP mutations are thought to cause disease by decreasing the stability of native PrP; there is strong evidence that this is an important general mechanism by which mutations can lead to protein-misfolding diseases[20,21]. But recent work on folded PrP indicates that at least some mutants have the same thermodynamic stability as wild-type PrP[22,23]. We suggest that some disease mutations enhance amyloidogenic processes by altering the forward folding and assembly pathway after energy barriers to unfolding have been overcome. □

Methods

Plasmid constructions. NM–GFP fusion constructs of R2E2 and RΔ2–5 were created by site-directed mutagenesis, using oligonucleotide primers and QuickChange Site-Directed Mutagenesis Kit (Stratagene). Primers for R2E2 were 5′-CAAGGTGGCTATCAACAGTACAATCCCCAAGGTGGCTATCAACAG-3′ and 5′-CTGTTGATAGCCACCTTGGGGATTGTACTGTTGATAGCCACCTTG-3′. Primers for RΔ2–5 were 5′-ATTCTGGGTACCAACCACAAGGTGGCCGTG-3′ and 5′-CACGGCCACCTTGTGGTTGGTACCCAGAAT-3′. The template plasmid for mutagenesis was p316CUP1-3SGFP^{SG}. To create p316CUP1-3SGFP^{SG}, the CUP1 promoter sequence from pCLUC (gift from D. Thiele)[24] was amplified by PCR and inserted into pRS316[25] at *Eco*RI/*Bam*HI sites using PCR primers 5′-CGGAATTCCCATTACCGACATTTGGGCGCT-3′ and 5′-CGGGATCCTGATTGATTGATTGATTGTACAGTTTG-3′. Wild-type NM was amplified by PCR and inserted into *Bam*HI/*Sac*I sites (primers: 5′-CGCGGATCCATGTCGGATTCAAACC-3′ and 5′-CGCGAGCTCACTAGCTAGTT-3′). GFP^{SG} was amplified by PCR using pJK19-1 (gift from P. Silver) as a template and inserted into *Sac*I/*Sac*II sites (primers: 5′-GATGAGCTCATGGCTAGCAAAGGAG-3′ and 5′-TCCCCGCGGTCATCCTTTGTATAGTTCATCCAT-3′).

A *SUP35* integrative vector was constructed with *SUP35* genomic sequences (5′ flanking region 1360 nt; 3′ flanking region 800 nt) inserted at *Xho*I/*Eco*RI and *Bam*HI/*Sac*II sites in pRS306[25], respectively, and was named pJLI-SUP35 (PCR primers for 5′ flanking region: 5′-CAGCAACTCGAGAAGATATCCATCAT-3′ and 5′-CGGAATTCTGTTGCTAGTGGGCAGAT-3′; primers for 3′ flanking region: 5′-CGGGATCCATTTCTTGCAAACATAAGTAAATGCAAAC-3′ and 5′-TCCCCGCGGTGAAAAGAGTCAGTGAGACGACGACGACT-3′). The DNA sequence encoding the Sup35 carboxy terminus (amino acids 124–685)

was amplified by PCR and inserted into pJLI-SUP35 at *Eco*RI/*Bam*HI sites (primers: 5′-CGGAATTCATGTCTTTGAACGACTTTCAAAAGC-3′ and 5′-CGCGGATCCTTACTCGGCAATTTTAAC-3′). The R2E2 and RΔ2–5 NPD sequences were then amplified and inserted into the plasmid at the *Eco*RI site, respectively (PCR primers: 5′-CGGAATTCATGTCGGATTCAAACCAAGG-3′ and 5′-CGGAATTCACCTTGAGACTGTGGTTGG-3′). The two constructs were then named pJLI-SUP35 R2E2 and pJLI-SUP35 RΔ2–5.

The non-His-tagged bacterial expression constructs of R2E2 and RΔ2–5 were constructed in the same way as the wild-type NM expression construct[26]. All constructs were confirmed by dideoxy nucleotide triphosphate sequencing.

Gene integration and replacement. Integrative constructs were digested with *Xba*I and transformed into 74-D694 [*PSI*$^+$] and [*psi*$^-$] strains. Transformants were selected on uracil-deficient (SD-Ura) medium and confirmed by genomic PCR. Recombinant excision events were selected on medium containing 5-fluoro-orotic acid[27]. Strains in which wild-type *SUP35* was replaced with the R2E2 and RΔ2–5 mutations were screened by PCR and confirmed by western blotting.

Spontaneous conversion from [*psi*$^-$] to [*PSI*$^+$]. To measure spontaneous conversion from [*psi*$^-$] to [*PSI*$^+$], red colonies carrying wild-type *SUP35*, R2E2 or RΔ2–5 were inoculated into liquid YPD medium and grown overnight at 30 °C. Cells were adjusted to equal densities, serially diluted and plated on to SD-Ade medium (5×10^2–10^8 cells per plate, depending on the strain). To confirm the presence of [*PSI*$^+$], colonies were patched onto YPD medium containing 5 mM guanidine-HCl, as described[16,28].

Analysis of NM-GFP cells. An exponential-phase isogenic pair of 74-D694 [*PSI*$^+$] and [*psi*$^-$] cells was induced to express the GFP-fusion proteins with 50 μM $CuSO_4$ at 30 °C. For fluorescence microscopy, cells were fixed with 1% formaldehyde after 4 and 20 h. For analysis of [*PSI*$^+$] induction, [*psi*$^-$] cells overexpressing GFP fusion proteins were serially diluted and spotted onto YPD and SD-Ade media after 4 and 20 h. The insolubility of Sup35 as the protein converts to the [*PSI*$^+$] state obviates standard immunoprecipitation procedures to identify protein complexes. For immunomagnetic purification of NM-GFP::Sup35 complexes, [*psi*$^-$] cells were suspended in protoplasting buffer (1 M sorbitol, 0.1 M EDTA, 50 mM dithiothreitol and 0.2 mg ml^{-1} zymolyase) after 4 h of induction and incubated at 37 °C for 1 h. Protoplasts were lysed in 50 mM Tris-HCl, pH 7.5, containing 5 mM $MgCl_2$, 10 mM KCl, 0.1 mM EDTA, 2 mM PMSF, 100 μg ml^{-1} ribonuclease A, 10 μg ml^{-1} leupeptin, 2 μg ml^{-1} pepstatin and 1 mM benzamidine. All samples were adjusted to 2 mg ml^{-1} total protein (Bio-Rad Bradford assay). Aliquots of each sample were then incubated with anti-GFP antibody (rabbit polyclonal; Clontech) or preimmune rabbit serum at 4 °C for 1 h. The antibody–protein complexes were isolated with magnetic beads (Dynabeads M-280 sheep anti-rabbit IgG; Dynal) and washed. Bound proteins were eluted with SDS-sample buffer, analysed by immunoblotting with anti-Sup35 antibody 1B, which recognizes the middle region of Sup35[2], and detected by chemiluminescence (ECL western blotting reagents; Amersham).

Congo-red binding. Congo-red binding was performed as described[29]. Denatured bacterial recombinant proteins were precipitated with 67% methanol and then redissolved in Congo red binding buffer (5 mM potassium phosphate, pH 7.4, 150 mM NaCl) to a final concentration of 10 μM. Proteins were then subjected to continuous slow rotation at a speed of 2.5 r.p.m. At indicated times, triplicate aliquots of each reaction were diluted to 2 μM protein and incubated with 10 μM Congo red. Congo-red binding was calculated as previously described[29] and plotted as the mean of triplicate determinations.

Received 23 March; accepted 9 June 1999.

1. Wickner, R. B. [URE3] as an altered URE2 protein: evidence for a prion analog in *Saccharomyces cerevisiae*. *Science* **264,** 566–569 (1994).
2. Patino, M. M., Liu, J. J., Glover, J. R. & Lindquist, S. Support for the prion hypothesis for inheritance of a phenotypic trait in yeast. *Science* **273,** 622–626 (1996).
3. Paushkin, S. V., Kushnirov, V. V., Smirnov, V. N. & Ter-Avanesyan, M. D. Propagation of the yeast prion-like [*psi*$^-$] determinant is mediated by oligomerization of the *SUP35*-encoded polypeptide chain release factor. *EMBO J.* **15,** 3127–3134 (1996).
4. Lindquist, S. Mad cows meet psi-chotic yeast: the expansion of the prion hypothesis. *Cell* **89,** 495–498 (1997).
5. Kretzschmar, H. A. *et al.* Molecular cloning of a human prion protein cDNA. *DNA* **5,** 315–324 (1986).
6. Kushnirov, V. V. *et al.* Nucleotide sequence of the *SUP2* (*SUP35*) gene of *Saccharomyces cerevisiae*. *Gene* **66,** 45–54 (1988).
7. Prusiner, S. B. & Scott, M. R. Genetics of prions. *Annu. Rev. Genet.* **31,** 139–175 (1997).
8. Chiesa, R., Piccardo, P., Ghetti, B. & Harris, D. A. Neurological illness in transgenic mice expressing a prion protein with an insertional mutation. *Neuron* **21,** 1339–1351 (1998).
9. Zhouravleva, G. *et al.* Termination of translation in eukaryotes is governed by two interacting polypeptide chain release factors, eRF1 and eRF3. *EMBO J.* **14,** 4065–4072 (1995).
10. Stansfield, I. *et al.* The products of the *SUP45* (eRF1) and *SUP35* genes interact to mediate translation termination in *Saccharomyces cerevisiae*. *EMBO J.* **14,** 4365–4373 (1995).
11. Ter-Avanesyan, M. D. *et al.* Deletion analysis of the *SUP35* gene of the yeast *Saccharomyces cerevisiae* reveals two non-overlapping functional regions in the encoded protein. *Mol. Microbiol.* **7,** 683–692 (1993).
12. Derkatch, I. L., Chernoff, Y. O., Kushnirov, V. V., Inge-Vechtomov, S. G. & Liebman, S. W. Genesis and variability of [*PSI*] prion factors in *Saccharomyces cerevisiae*. *Genetics* **144,** 1375–1386 (1996).
13. Glover, J. R. *et al.* Self-seeded fibers formed by Sup35, the protein determinant of [*PSI*$^+$], a heritable prion-like factor of *S. cerevisiae*. *Cell* **89,** 811–819 (1997).
14. DePace, A. H., Santoso, A., Hillner, P. & Weissman, J. S. A critical role for amino-terminal glutamine/asparagine repeats in the formation and propagation of a yeast prion. *Cell* **93,** 1241–1252 (1998).
15. Chernoff, Y. O., Lindquist, S. L., Ono, B., Inge-Vechtomov, S. G. & Liebman, S. W. Role of the chaperone protein Hsp104 in propagation of the yeast prion-like factor [*psi*$^+$]. *Science* **268,** 880–884 (1995).
16. Tuite, M. F., Mundy, C. R. & Cox, B. S. Agents that cause a high frequency of genetic change from [*psi*$^+$] to [*psi*$^-$] in *Saccharomyces cerevisiae*. *Genetics* **98,** 691–711 (1981).
17. Chernoff, Y. O., Derkach, I. L. & Inge-Vechtomov, S. G. Multicopy *SUP35* gene induces de-novo appearance of *psi*-like factors in the yeast *Saccharomyces cerevisiae*. *Curr. Genet.* **24,** 268–270 (1993).
18. Paushkin, S. V., Kushnirov, V. V., Smirnov, V. N. & Ter-Avanesyan, M. D. *In vitro* propagation of the prion-like state of yeast Sup35 protein. *Science* **277,** 381–383 (1997).
19. Goldmann, W., Chong, A., Foster, J., Hope, J. & Hunter, N. The shortest known prion protein gene allele occurs in goats, has only three octapeptide repeats and is non-pathogenic. *J. Gen. Virol.* **79,** 3173–3176 (1998).
20. McCutchen, S. L., Lai, Z., Miroy, G. J., Kelly, J. W. & Colon, W. Comparison of lethal and nonlethal transthyretin variants and their relationship to amyloid disease. *Biochemistry* **34,** 13527–13536 (1995).
21. Booth, D. R. *et al.* Instability, unfolding and aggregation of human lysozyme variants underlying amyloid fibrillogenesis. *Nature* **385,** 787–793 (1997).
22. Swietnicki, W., Petersen, R. B., Gambetti, P. & Surewicz, W. K. Familial mutations and the thermodynamic stability of the recombinant human prion protein. *J. Biol. Chem.* **273,** 31048–31052 (1998).
23. Liemann, S. & Glockshuber, R. Influence of amino acid substitutions related to inherited human prion diseases of the thermodynamical stability of the cellular prion protein. *Biochemistry* **38,** 3258–3267 (1999).
24. Thiele, D. J. ACE1 regulates expression of the *Saccharomyces cerevisiae* metallothionein gene. *Mol. Cell. Biol.* **8,** 2745–2752 (1988).
25. Sikorski, R. S. & Hieter, P. A system of shuttle vectors and yeast host strains designed for efficient manipulation of DNA in *Saccharomyces cerevisiae*. *Genetics* **122,** 19–27 (1989).
26. Serio, T. R., Cashikar, A. G., Moslehi, J. J., Kowal, A. S. & Lindquist, S. L. The yeast prion [*PSI*$^+$] and its determinant, Sup35p. *Methods Enzymol.* (in the press).
27. Ausubel, F. M. *et al. Current Protocols in Molecular Biology* (Greene Publishing Associates/Wiley Interscience, New York, 1991).
28. Derkatch, I. L., Bradley, M. E., Zhou, P., Chernoff, Y. O. & Liebman, S. W. Genetic and environmental factors affecting the *de novo* appearance of the [*PSI*$^+$] prion in *Saccharomyces cerevisiae*. *Genetics* **147,** 507–519 (1997).
29. Klunk, W. E., Pettegrew, J. W. & Abraham, D. J. Two simple methods for quantifying low-affinity dye-substrating binding. *J. Histochem. Cytochem.* **37,** 1293–1297 (1989).

Acknowledgements. We thank A. Kowal for technical assistance on electron microscopy, A. Cashikar for assistance with the circular dichroism study, and H. True, T. Serio, S. Uptain, T. Scheibel, L. Li and J. Ma for comments on the manuscript. This work was supported by a grant from the National Institutes of Health and the Howard Hughes Medical Institute.

Correspondence and requests for materials should be addressed to S.L. (e-mail: s-lindquist@uchicago.edu).

Skeletal muscle hypertrophy is mediated by a Ca^{2+}-dependent calcineurin signalling pathway

Christopher Semsarian*, Ming-Jie Wu*, Yue-Kun Ju†, Tadeusz Marciniec*, Thomas Yeoh*, David G. Allen†, Richard P. Harvey*‡ & Robert M. Graham*‡

** Victor Chang Cardiac Research Institute, St Vincent's Hospital, New South Wales, 2010, Australia*
† Department of Physiology, University of Sydney, New South Wales, 2006, Australia
‡ School of Biochemistry and Molecular Genetics, University of New South Wales, New South Wales 2033, Australia

Skeletal muscle hypertrophy and regeneration are important adaptive responses to both physical activity and pathological stimuli[1]. Failure to maintain these processes underlies the loss of skeletal muscle mass and strength that occurs with ageing and in myopathies[2]. Here we show that stable expression of a gene encoding insulin-like growth factor 1 (IGF-1) in C2C12 skeletal muscle cells, or treatment of these cells with recombinant IGF-1 or with insulin and dexamethasone, results in hypertrophy of